Title

PRPs localized to the middle lamellae are required for cortical tissue integrity in Medicago truncatula roots

Journal

Plant Molecular Biology, 102(6)

ISSN

0167-4412

Authors

Erickson, B Joy
Staples, Nathan C
Hess, Nicole
et al.

Publication Date

2020-04-01

DOI

10.1007/s11103-019-00960-5

Peer reviewed

Plant Molecular Biology (2020) 102:571–588
https://doi.org/10.1007/s11103-019-00960-5

PRPs localized to the middle lamellae are required for cortical tissue integrity in *Medicago truncatula* roots

B. Joy Erickson[2,3] · Nathan C. Staples[1,4] · Nicole Hess[1] · Michelle A. Staples[1] · Christian Weissert[1,5] · Ruth R. Finkelstein[1] · James B. Cooper[1,2]

Received: 31 August 2019 / Accepted: 30 December 2019 / Published online: 11 January 2020

Abstract

Key message **A family of repetitive proline-rich proteins interact with acidic pectins and play distinct roles in legume root cell walls affecting cortical and vascular structure.**

Abstract A proline-rich protein (PRP) family, composed of tandemly repeated Pro-Hyp-Val-X-Lys pentapeptide motifs, is found primarily in the Leguminosae. Four distinct size classes within this family are encoded by seven tightly linked genes: *MtPRP1*, *MtPRP2* and *MtPRP3*, and four nearly identical *MtPRP4* genes. Promoter fusions to β-glucuronidase showed strong expression in the stele of hairy roots for all 4 *PRP* genes tested, with additional expression in the cortex for *PRP1, PRP2* and *PRP4*. All except *MtPRP4* are strongly expressed in non-tumorous roots, and secreted and ionically bound to root cell walls. These PRPs are absent from root epidermal cell walls, and PRP accumulation is highly localized within the walls of root cortical and vascular tissues. Within xylem tissue, PRPs are deposited in secondary thickenings where it is spatially exclusive to lignin. In newly differentiating xylem, PRPs are deposited in the regularly spaced paired-pits and pit membranes that hydraulically connect neighboring xylem elements. Hairpin-RNA knock-down constructs reducing PRP expression in *Medicago truncatula* hairy root tumors disrupted cortical and vascular patterning. Immunoblots showed that the knockdown tumors had potentially compensating increases in the non-targeted PRPs, all of which cross-react with the anti-PRP antibodies. However, PRP3 knockdown differed from knockdown of PRP1 and PRP2 in that it greatly reduced viability of hairy root tumors. We hypothesize that repetitive PRPs interact with acidic pectins to form block-copolymer gels that can play distinct roles in legume root cell walls.

Keywords Proline-rich proteins (PRPs) · Medicago · Root cell walls · Pectins · Root structure

Introduction

The extracellular matrices surrounding each plant cell have complicated architectures that dynamically change during development and in response to external stimuli. By regulating the deposition and assembly of individual wall components, plant cells construct walls that tightly adhere neighboring cells to one another and control the rate and direction of cellular growth. During cellular differentiation, cell wall structure can become highly specialized ultimately contributing to the physiology of most differentiated tissues. These roles include functioning as a barrier that protects plant cells against invasion by pathogens, enabling cell–cell communication within the plant, and preventing water loss in aerial organs.

Plant cell walls are exceptionally rich in structural carbohydrates, including cellulose, and hemicellulosic and pectic

Electronic supplementary material The online version of this article (https://doi.org/10.1007/s11103-019-00960-5) contains supplementary material, which is available to authorized users.

✉ Ruth R. Finkelstein
finkelst@lifesci.ucsb.edu

[1] Molecular, Cellular, and Developmental Biology Department, University of California at Santa Barbara, Santa Barbara, CA 93106, USA

[2] Biomolecular Science and Engineering Program, University of California at Santa Barbara, Santa Barbara, CA 93106, USA

[3] Present Address: Biological Sciences Department, Santa Rosa Junior College, Santa Rosa, CA 95401, USA

[4] Present Address: Biological Sciences Department, Cañada College, Redwood City, CA 94061, USA

[5] Present Address: Biology Department, Universität Hamburg, 22609 Hamburg, Germany

polysaccharides. Recent research into water-polysaccharide interactions in the primary cell wall of *Arabidopsis* supports the single network model of cell wall structure (White et al. 2014): the idea that all three types of polysaccharides form a single network and share load bearing responsibilities (Wang et al. 2012). Approximately 5–10% of cell wall mass is made up of proteins, both enzymatic and structural (Cassab 1998). Several cell wall proteomic studies in *Arabidopsis* have identified over 500 proteins which have subsequently been organized into nine functional categories (as reviewed in Albenne et al. 2013). Cell wall proteomic studies have also been performed in the legume alfalfa (*Medicago sativa*), where 272 proteins were identified based on sequence homology to the *Medicago truncatula* genome (Verdonk et al. 2012; Watson et al. 2004). Further proteomic analyses suggest that as little as 1–2% of proteins in plant cell walls serve structural roles, depending on the species and the nature of the analysis performed (Albenne et al. 2013; Verdonk et al. 2012).

Structural proteins in both plants and animals share two common characteristics: they are generally repetitive and contain above average proportions of 4-trans-hydroxy-L-proline (Hyp) and/or glycine (Keller 1993). Since the discovery of cell wall "Extensin" nearly 60 years ago, Hyp-rich wall components have been identified in many different plant species, and shown to fall into discrete structural classes that include the arabinogalactan-protein proteoglycans, the "extensin" Hyp-rich glycoproteins (HRGPs), the repetitive proline-rich-proteins (PRPs), and chimeric molecules containing a PRP or HRGP domain, fused to Cys-rich or Leu-rich domain. HRGPs and PRPs sequences invariably include a high content of tandemly repeated peptide motifs, sharing the tandem-repeat protein (TRP) architecture with many biostructural proteins found throughout nature (e.g. collagen). A bioinformatics approach looked specifically at secreted Pro-rich structural proteins in plants and identified five tandem repeat motif superclasses that differ from the previously defined groups: PELPKs, seed storage proteins, extensins + hybrid extensins, PEPKs + PEHKs + PHEKs, and PRPs + hybrid PRPs (Newman and Cooper 2011).

Cell wall PRPs have been well-characterized in legumes. Legume PRP gene products differ from those in other species in that they consist of conserved N-terminal signal peptides fused to secreted proteins composed almost entirely of tandemly-repeated pentapeptides with the sequence POVXK, where O represents Hyp and X is most commonly Glu or Tyr or His (Averyhart-Fullard et al. 1988; Bradley et al. 1992; Datta et al. 1989; Hong et al. 1990; Kleis-San Francisco and Tierney 1990; Lindstrom and Vodkin 1991; Wilson et al. 1994). By contrast, PRPs in *Arabidopsis* are exclusively found as chimeric wall proteins comprised of a signal peptide followed by one repetitive and one non-repetitive domain and therefore don't fit the definition of cell wall PRPs described previously (Fowler et al. 1999). Expression of legume PRP genes is organ- and tissue-specific, and has been shown to be differentially regulated both during shoot development and in response to various external stimuli (Creelman et al. 1992; Datta et al. 1989; Hong et al. 1989; Suzuki et al. 1993a, b; Wyatt et al. 1992; Ye et al. 1991). Legume PRP genes are also expressed in roots (Hong et al. 1989; Suzuki et al. 1993a, b) and closely related PRP sequences were identified as host early nodulin genes expressed during the symbiotic response of legume roots to rhizobial bacteria and mycorrhizal fungi (Allison et al. 1993; Franssen et al. 1987; Journet et al. 2001; Löbler and Hirsch 1993; Perlick and Pühler 1993; Pichon et al. 1992; Scheres et al. 1990; Wilson et al. 1994). Following secretion into legume cell walls, soluble PRPs can be oxidatively cross-linked to form an insoluble network that may constrain cell elongation and strengthen cell walls both in lignified tissues and during plant defense against external stresses (Bradley et al. 1992; Otte and Barz 1996, 2000). The repeat motif of the strictly defined PRPs yields an abundance of Lys residues that suggests these proteins might interact ionically with acidic cell wall pectins (Marcus et al. 1991), an assertion that is supported in part by the observation that some PRPs are extractable with high salt (Datta et al. 1989).

Based on the available evidence, it is likely that PRPs play important roles in the architecture of root cell walls during cell growth and differentiation and during plant–microbe interactions. The fact that this family of cell wall proteins is restricted to legumes suggests a legume-specific function and it has been proposed that they are involved in cell wall remodeling during or after nodule formation (Wilson et al. 1994). Interestingly, they are not the only known legume-specific cell wall proteins (Schultz and Harrison 2008). Although studies of localization and developmental or other regulation are suggestive of roles for these proteins, no specific functions have been ascribed to any particular legume cell wall PRP, and little is yet known about the function of PRPs in wall architecture. To complement our earlier studies of symbiosis-specific PRPs, we characterized the major root PRPs from the model legume *M. truncatula*, and used transcriptional β-glucuronidase fusions and RNAi knock-down experiments to investigate their localization and function in root development. Our data support the hypothesis that PRP1 and PRP3 play non-redundant roles in root development and are specifically involved in maintaining the structural integrity of the root cortex.

Materials and methods

Plant material

Seeds of *Medicago sativa* cv. GT13 (Ferry Morse Seed Co., Mountain View, CA) and *M. truncatula* cv. Jemalong

(Purkiss seeds, Newcastle, Australia) were surface sterilized, then imbibed and germinated as described in (Garcia et al. 2006). Seedlings were planted in a single row on NGM media (Supplementary Methods) on square agar plates as described in (Barker et al. 2006).

Generating and selecting transgenic *M. truncatula* hairy roots

Inoculation was performed via hypocotyl wounding using a 27G needle coated with a single colony of the desired *A. rhizogenes* line. Kanamycin selection of excised hairy roots was performed 14–21 days after inoculation, in 0.5 × MS30 (Murashige and Skoog 1962) liquid culture supplemented with 500 µg ml^{-1} Claforan as described in (Boisson-Dernier et al. 2001).

Transient expression in *Nicotiana benthamiana*

PRP overexpression constructs were transformed into *Agrobacterium tumefaciens* strain GV3101, then combined with GV3101 expressing the P19 protein of tomato bushy stunt virus to suppress gene silencing in co-transformed *N. benthamiana,* as described in (Sainsbury and Lomonossoff 2014).

Generation of antibodies against synthetic peptide motifs

Synthetic peptides with the sequence $(ProHypValHisLys)_3ProHypCys$ (= "POVHK peptide") and $(ProHypValTyrLys)_3ProHypCys$ (= "POVYK peptide") were synthesized using fMOC chemistry on an ABI Model 3000 peptide synthesizer, then deprotected and purified using HPLC on a C18 column eluted with a H_2O:acetonitrile gradient. The identity of the purified peptides was verified by mass spectrometry. The POVHK peptide was then conjugated to keyhole limpet hemocyanin and used to immunize New Zealand white rabbits. Affinity purification is described in Supplementary Methods.

Cloning of PRP3

Alignment of EST sequence data containing the characteristic pentapeptide repeats revealed a 1305 bp open reading frame encoding a novel PRP gene of distinct size. PCR primers were designed to the 5′ and 3′ ends of the open reading frame of *MtPRP*3. Gradient touchdown PCR was used to optimize specificity and annealing.

Protein extraction

Boiling SDS extraction

Fresh tissue was ground on ice in 4–10 µl extraction buffer per mg of wet weight of tissue. Extraction buffer was 2% SDS, 25 mM Tris–Cl pH 6.8, 0.5% BME or 2.5 mM DTT, and one protease inhibitor cocktail tablet for every 20 ml. An equal volume of hot 4% SDS was used to rinse the grinder and pooled with the extract. The samples were boiled for 3 min and then spun in a microcentrifuge at top speed for 15 min. Extractable soluble proteins were collected in the supernatants.

Cell wall preparation

Frozen tissue was thawed 1–2 min. on ice, then homogenized in extraction buffer (25 mM Tris–Cl, pH 8.0, 5 mM ascorbate, 5 mM DTT, 4 mM Na_2SO_4, 1 mM PMSF) in a chilled Duall grinder, using 5 ml buffer per gram tissue. The homogenate was centrifuged for 10 min. at 1700×*g*. The supernatant was retained as the "cytoplasmic" fraction. The cell wall pellet was washed once with extraction buffer plus 0.1% NP40, then 5 washes with 4 mM Na_2SO_4 and 1 wash with cold water, centrifuging at 1700×*g* after each wash. Soluble PRPs were extracted from the cell wall preparations by 1 h incubation at 4 °C in salt (2 M NH_4OAc, 5 mM ascorbate at 1 ml per gram fresh weight), followed by centrifuging 10 min. at 1000×*g*. Salt-extractable proteins were in the supernatant. The pellet was re-extracted by boiling in 2% SDS, then re-centrifuged. Alternatively, the SDS extraction was performed without doing a prior salt extraction.

Whole cell elution of cell wall proteins

The biophysical properties of PRPs at different pHs or salt concentrations were used to separate them from the cell wall components by overcoming charge–charge interactions. Whole root tissues were washed successively with 50 mM triethanolamine at pH 9, 10, 11 and 12.

Extract protein concentrations were determined by BCA assays (Pierce Chemical Co., Rockford, IL), Bradford assays (Bio-Rad Laboratories, Hercules, CA), or "Dot Bradford" method, using Coomassie R-250 solutions generally used for staining gels to detect the amount of protein in 1 µl of a protein sample compared to a standard curve of BSA in a range from 0.1 to 5 mg ml^{-1}.

Immunoblotting

SDS-PAGE was performed with 2–5 µg of total extracted protein per sample on 10% or 12% acrylamide resolving gels, with prestained protein molecular weight standards.

Following electrophoresis, proteins were electroblotted to nitrocellulose membranes in a Tris/glycine buffer (pH 8.3) containing 20% methanol. Filters were blocked in 5% non-fat dry milk in Tris-buffered saline (TBS) for at least 2 h, washed four times with TBS, and incubated with 50 ng ml^{-1} affinity purified rabbit antibodies. HK-specific Ab383 was applied to blots at 200 ng ml^{-1}. Immunoreactive proteins were detected by either Supersignal West Pico reagents (Pierce, Rockford, IL) following incubation with peroxidase-conjugated secondary antibodies or Odyssey imaging system (LI-COR Biosciences, Lincoln, NE) detection of fluorescently labeled secondary antibodies. Equivalent loading of protein samples on all immunoblots was verified by either Coomassie Blue staining of gels loaded with identical protein samples or Ponceau staining of the proteins transferred to the filters.

Immunohistochemistry

Plant tissue was fixed in 4% paraformaldehyde in an isotonic solution (50 mM KPi, pH 6.8) overnight at 4 °C with gentle agitation in excess volume to tissue ratio**.** Tissue was cut into desired segments and embedded in 65 °C 5% low melting point agarose with 0.02% NaAzide to prevent contamination. The tissue was gently swirled in the warm agarose to ensure complete embedding.

A Vibratome was used to produce 50 or 100 µm thick sections, that were then blocked 18–24 h at 4 °C in 2.5 ml dilution buffer "DB" (filter sterile, 1/50 sheep serum, 1% BSA, 0.02% Na Azide, 1 × PBS), washed 2 × 10 min in PBS, then incubated 20–24 h in 1 ml 200 ng ml^{-1} Primary Antibody Ab383 (POV-K) in DB. The secondary antibody, goat anti-rabbit IgG conjugated with Texas Red or CY3 (Jackson ImmunoResearch Laboratories, West Grove, PA), was preabsorbed to plant tissue 3 h before use at 37 °C at 10 µg ml^{-1} in DB. The hairy root tissue was removed via centrifugation followed by sterile filtration before using the secondary antibody. Sections were washed 2 × 30 min in PBS before incubation in secondary antibody (1 µg ml^{-1}) in DB for 12–18 h in the dark at 4 °C with gentle agitation. Following immunostaining, the sections were washed 4 × 15 min in 1 × PBS, mounted on slides in glycerol containing 5% (w/v) n-propyl gallate (Hale and Matsumoto 1993).

Screening BAC Library

The MT_ABb (barrel medic) BAC Library filter set was purchased from Clemson University Genomic Institute (CUGI) (Gamas et al. 2006; Nam et al. 1999). Filters were hybridized to a radiolabeled probe derived from pooled PCR products amplified from PRP1–3 cDNA plasmid clones. Background hybridization to identify locations of all BAC spots was achieved using EcoRI linearized pBR329 as template for a second probe. The probes were labeled with [alpha-^{32}P] dCTP via random priming using 30–100 ng of probe template (Feinberg and Vogelstein 1983). Unincorporated nucleotides were removed via spin column chromatography.

All hybridization and wash steps were carried out in a HybAid Mini Hybridization Oven. Filters were pre-hybridized in Church Hybridization Buffer (Church and Gilbert 1984) at 64 °C for at least 1 h. The probes were mixed 10:1 (PRP:pBR329) and hybridized overnight at 64 °C. Filters were washed at 63 °C, first with 2 × SSC, 0.1% SDS for at least 40 min, then 1 × SSC, 0.1% SDS for at least 1 h. Filters were exposed to a Phosphor Screen, then developed using a Molecular Imager System (Bio-Rad, Hercules, CA), and further analyzed using BioRad's Quantity One 1D Analysis Software.

Filter hybridization results were analyzed using Hybdecon Freeware (https://www.windows8downloadsfree.com/hybdecon/win8+kmclk.html), software which matches user-called spots on a filter with individual clones in the library.

Screening BAC clones

BAC DNA was isolated via alkaline lysis and then further concentrated via ethanol precipitation. Restriction digests of BAC DNA were performed using enzymes that do not cut within PRP1–3. Following agarose gel electrophoresis, Southern blot hybridizations were performed using probes generated by random priming of PRP templates with digoxigenin-11-dUTP via the DIG DNA Labeling and Detection Kit (Roche Life Science, Indianapolis, IN), according to manufacturer's protocol.

Sequences of the PRP genes are available with the following GenBank accession numbers: PRP1 (MN396797), PRP4C (MN396798), PRP4B (MN396799), PRP4-pseudogene (MN396800), PRP3 (MN396801), PRP4D (MN396802).

Transgene construction

Promoter fusions

BAC DNA was digested with HindIII or BamHI, and fragments of the same size as those hybridizing to the PRP probe on the BAC Southern blots were subcloned into pBluescript SK vector (Stratagene) and transformed into TOP10 Electrocompetent *Escherichia coli* (Thermofisher) by electroporation. Subclones were screened for PRP homology via Southern and individual PRP-positive subclones sequenced. PRP promoter-GUS fusions were constructed by PCR amplification of upstream sequences using either ExTaq DNA polymerase (Takara, Clontech Laboratories Inc., Mountain View, CA) or Taq DNA polymerase (New England Biolabs, Ipswich, MA), followed by either LR Clonase recombination

into pGWB433 (Nakagawa et al. 2007) or ligation into pBI101 (Jefferson et al. 1987).

The PRP1 and PRP3 promoters (1353 bp and 861 bp upstream of the respective start codons) were subcloned into pBI101. A 2.4 kb fragment upstream of PRP2 was amplified from BAC DNA and then recombined into the pDONR221 vector (ThermoFisher Scientific, Wilmington, DE) followed by recombination into the pGWB433 vector (Nakagawa et al. 2007). The PRP4 promoter was subcloned as a 4.7 kb SalI–HindIII fragment, including the first 5 codons of PRP4, from a genomic clone described in (Wilson et al. 1994). After verifying the cloned constructs via diagnostic restriction digest, each was transformed into *Agrobacterium rhizogenes* and *A. tumefaciens* via liquid N_2 freeze/thaw (Wise et al. 2006).

RNAi knockdown of PRP expression

Target sequences from the 3′ UTR of each PRP target were amplified from genomic DNA using PCR primers with the addition of attB sites for use with Gateway Recombination Cloning. The amplified PCR product was recombined into pDONR221 using BP Clonase, and subsequently recombined into the inverted hairpin repeat of the destination vector, pHellsgate12 (Wesley et al. 2001) by LR Clonase.

PRP over expression

Each of the PRPs were cloned into pGA643, a binary vector with a cloning site downstream of the CaMV 35S promoter. Primers were designed to add a HindIII and a ribosome binding site (RBS) to the 5′ end of the open reading frame and a Bgl II restriction site to the 3′ end to facilitate directional cloning. Sequence-verified constructs were transferred to *A. rhizogenes* strain A4 through transconjugation using a helper plasmid pRK2031 (Wise et al. 2006).

Generating and imaging *M. truncatula* GUS-stained hairy root cross sections

Following kanamycin selection of transfected *M. truncatula* hairy roots on solid 0.5 × MS30 media, 0.3 to 0.5 cm pieces of root were excised and submerged in 50–60 °C water to prepare for embedding in warm (50–60 °C) agarose, as described above. After the agarose solidified, pieces of agarose containing root were cut into pyramids with a clean razorblade to ensure vertical orientation of root.

Tissues or agarose blocks were submerged in GUS staining buffer (Jefferson et al. 1987), vacuum infiltrated for 10–15 min, and then allowed to incubate at 37 °C overnight. Agarose blocks for cross sections were briefly destained with nanopure water before sectioning.

100 µm cross sections were cut in an ice water bath using a Vibratome (Leica Biosystems, Buffalo Grove, IL) with a speed of 1 and a vibrating speed of 7. Sections were mounted in water and visualized immediately using an Olympus CKX41 inverted microscope (Olympus, Center Valley, Pennsylvania). Images were captured using an Infinity 2 camera and Infinity Analyze software (Lumenera, Ottawa, Ontario, Canada) and scale bars were added using ImageJ (https://www.imagej.nih.gov).

Results

The MtPRP family

Three *M. truncatula* PRPs have been described in the literature to date (MtPRP1, 2 and 4) (Wilson and Cooper 1994; Wilson et al. 1994). MtPRP1 and MtPRP2 are homologs of SbPRP1 and 2, respectively, and are composed almost entirely of PPVYK and PPVEK repeats flanked by a highly conserved signal peptide, and conserved N- and C-terminal domains (44 and 60 amino acid residues long, respectively). MtPRP1 is more hydrophobic (PPVVK repeats), less acidic (fewer PPVEK repeats), and smaller than MtPRP2. They also share homology with several *M. truncatula* early nodulin gene products (Table 1; Suppl. Fig. 1). MtPRP4 is the largest PRP and contains a 527-amino acid repetitive proline-rich domain composed of three repetitive pentapeptide motifs arranged into two decapeptide repeats: PPVEKPPVHK and PPVEKPPVYK. The fraction of tyrosine-containing repeats varies from roughly 21% in PRP4 to greater than 60% in PRP1, resulting in vastly different potential for cross-linking of these PRPs via isodityrosine links (Table 2) (Fry 1982). The presence of multiple hybridizing fragments on genomic Southern blots (Wilson et al. 1994) indicated that additional PRP genes were likely. However, due to the repetitive nature of the PRP family both at the protein and gene level, they were absent from available *M. truncatula* genomic data.

Since cell wall PRPs have a tandem repeat protein (TRP) architecture, we analyzed ~ 135,000 publicly available *M. truncatula* sequences using XSTREAM, a bioinformatics tool that effectively identifies and models the architecture of TRPs from protein sequence datasets (Newman and Cooper 2007). Alignment of EST sequence data containing the characteristic PPVXK penta-peptide found in PRP family members revealed a 1305 base pair open reading frame encoding a novel PRP gene of distinct size. Similar to PRP1 and PRP2, this new PRP is composed primarily of alternating PPVYK and PPVEK repeats, with a signal peptide 77% identical to that of PRP1, but more diverse proline-rich pentapeptide repeats at N- and C-termini of the mature protein. PCR amplification from genomic and cDNA followed by

Table 1 Overview of most common proline rich pentapeptide repeats found in the PRPs showing differences between cDNA (or EST), BAC, and v4.0 sequence data. #=total pentapeptides beginning with PP

PRP	Source	PPVEK	PPVVK	PPVYK	PPIYK	PPVHK	PPLHK	PPHKE	#
PRP1	cDNA	7	4	22	0	0	0	0	36
	BAC	7	4	22	0	0	0	0	36
	v4.0	8 (+1)	4	24 (+2)	0	0	0	0	38
PRP2	cDNA	31	0	33	2	0	0	0	69
	BAC	–	–	–	–	–	–	0	–
	v4.0	25 (−6)	0	28 (−5)	1 (−1)	0	0	0	56
PRP3	EST	25	0	24	9	0	0	0	81
	BAC	25	0	24	9	0	0	0	81
	v4.0	20 (−5)	0	18 (−6)	9	0	0	0	70
PRP4A	gDNA	32	0	8	1	20	5	0	78
	BAC	–	–	–	–	–	–	0	–
	v4.0	–	–	–	–	–	–	0	–
	Pseudogene	13	0	6	0	8	0	0	33
	PRP4B	24	0	8	1	16	4	0	66
	PRP4C	32	0	8	1	17	4	0	75
	PRP4D	32	0	8	1	17	4	0	73
ENOD12						5		5	9

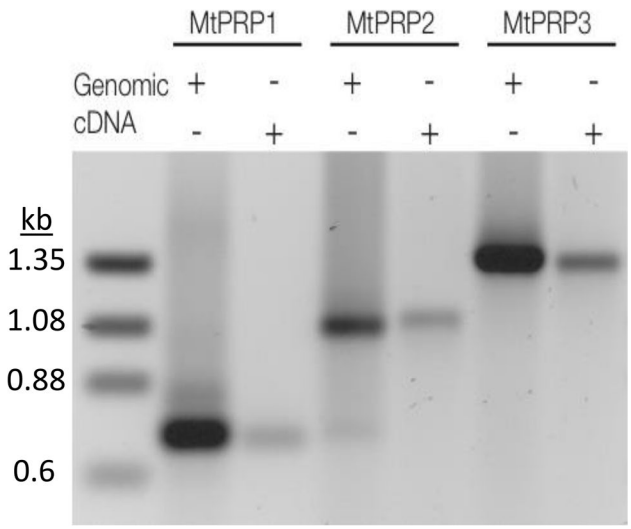

Fig. 1 PCR and RT-PCR amplification of genomic and cDNA PRP products. Amplified fragments encompass the ORF for each gene

DNA sequencing confirmed the existence of this predicted gene, designated MtPRP3. Similar analyses of MtPRPs 1 and 2 indicate that all of these PRP family members lack introns (Fig. 1). Previously, sequencing of a genomic clone for MtPRP4 also showed no introns in this family member (Wilson et al. 1994).

MtPRP1, *MtPRP2* and *MtPRP3* are the major proline-rich protein genes expressed in *M. truncatula* root cell walls

We have investigated expression of the *MtPRP* gene family in roots by a combination of analyses of RNA blots, RT-PCR and presence in EST libraries derived from specific source tissues. Hybridization with the coding sequence detects all family members, revealing two highly expressed transcripts in roots and two additional larger transcripts appearing in nodules where the major root-expressed transcripts are less abundant (Wilson et al. 1994). High stringency hybridization to a gene-specific probe showed that *MtPRP4* expression was limited to nodules. The sizes of the major root-expressed *M. truncatula* transcripts (~0.95 kb and ~1.4 kb)

Table 2 Comparison of tyrosine-containing repeat content of PRP family members

	PRP1	PRP2	PRP3	PRP4A	PRP4B	PRP4C	PRP4D
Y repeats	24	37	43	23	21	22	21
% Y repeats	63.2	52.1	51.2	21.5	22.6	21.4	21.0
Crosslinking ability	0.343	0.149	0.124	0.041	0.049	0.042	0.039
pI	9.87	9.70	9.44	9.76	9.75	9.75	9.76

"Y repeats" indicates number of pentapeptide repeats that contain tyrosine. "Crosslinking ability" is the percent of Y-containing repeats divided by the length of the mature PRP

correspond well with the sizes of the *MtPRP1* and *MtPRP2* cDNA clones (942 bp and 1436 bp) (Wilson and Cooper 1994). *MtPRP3* is also expressed in roots and corresponds to an approximately 1.7 kb transcript.

Both major transcripts are also detectable in green hypocotyls and symbiotic root nodules. Although no homologous transcripts were detected in either medic leaves or cotyledons using RNA blotting experiments (data not shown), ESTs for both *MtPRP1* and *MtPRP2* were present in libraries produced from leaves and, to a lesser extent, flowers (Fig. 2). *MtPRP3* ESTs were present in libraries from nodules, roots, and germinating seeds. Over 80% of *MtPRP4* ESTs were found in a library derived from immature pod tissue; the rest were derived from libraries produced from nodules, flowers and germinating seeds.

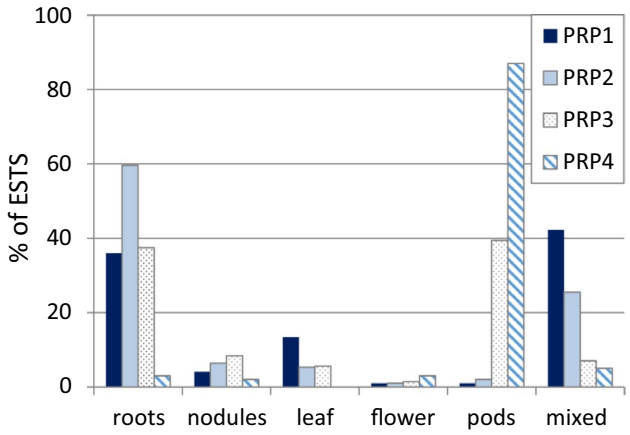

Fig. 2 Distribution of PRP transcripts in EST database. PRP cDNA sequences were used as queries in BLAST searches of EST databases, and individual clones were classified according to the tissue/organ source for the library. "Roots" represent a combination of many developmental stages, suspension cultures, and treatments including inoculation with a variety of symbionts, nematodes, and starvation for nitrogen or phosphate

The accumulation of cell wall PRPs corresponding to these MtPRP gene products was examined in medic seedlings using immunoblotting experiments. As shown in Table 1, secreted proline-rich protein domains identified in *M. truncatula* consist almost entirely of PPVXK pentapeptides, where X represents Y, E, V, H, or N. The sequence of SbPRP2 is 98% identical to the predicted sequence of MtPRP2 over 200 amino acids, and antiserum raised against purified SbPRP2 was previously shown to recognize both PRP1 and PRP2 in soybean (Lindstrom and Vodkin 1991). Immunoblots using this antibody to compare PRP accumulation in different root zones showed soluble products first appearing in the emerging root hair zone, and increasing accumulation in cell wall fractions of older roots (Fig. 3a). In addition to the major products appearing early, a "ladder" of less abundant products were detected in older roots. Based both on the sequence similarity between MtPRP1 and the SbPRPs, and on the contiguity hypothesis proposed to encode prolyl hydroxylation (Duruflé et al. 2017; Kieliszewski and Lamport 1994), every second proline in each pentapeptide repeat is predicted to be hydroxylated. Anti-PRP antibodies were generated against a synthetic pentapeptide repeat found in the nodulin MtPRP4 and were affinity-purified by binding to an immobilized $(POVYK)_3$ peptide sequence found in both PRP1 and PRP2. These antibodies (Ab383) recognized two major immunoreactive polypeptides in extracts of medic seedling tissues, migrating as 33 kDa and 50 kDa polypeptides when compared to globular protein size standards (Fig. 3b). Consistent with the EST data, PRPs were also detected in leaf tissue. A third lesser abundant PRP, migrating at ~ 65 kDa, was also observed in nodules and seedling extracts, though the abundance of this immunoreactive protein was highly variable. An additional higher

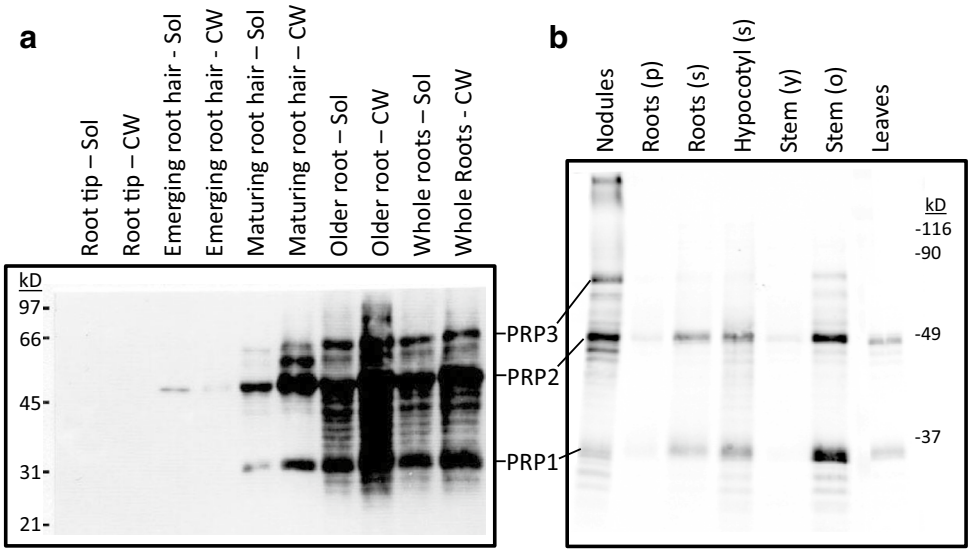

Fig. 3 Immunoblots of PRP-related proteins in *M. truncatula* organs. **a** Proteins cross-reacting with anti-sbPRP2 in soluble (Sol) and SDS-extractable cell wall (CW) fractions from indicated root zones of 4 days old seedlings. **b** Proteins cross-reacting with Ab383 (anti-POVH/YK) in organs of seedlings and 1 month old *M. truncatula* plants. Roots (p) = pooled developmental stages, (s) = seedling, (y) = young, (o) = old. All lanes contain 2 µg protein

molecular weight PRP was prevalent in seed pods (Suppl. Fig. 2).

The three major immunoreactive MtPRPs migrated with sizes (33 kDa, 50 kDa, and 65 kDa) much larger than the sizes of MtPRP1, MtPRP2, and MtPRP3 predicted from cDNA sequences (23 kDa, 42 kDa, and 50 kDa, respectively). This might be expected for polypeptides with very high proline content (Ziemer et al. 1982), and was observed for the homologous soybean PRPs (Lindstrom and Vodkin 1991), yet several alternative explanations exist. One possibility is that the soluble PRPs may represent the products of other, as yet uncharacterized PRP genes. To determine the expected migration for the 3 major MtPRPs, cDNAs for each were transiently over-expressed in leaves of *N. benthamiana,* which lacks genes encoding these legume-specific PRPs, and protein extracts were compared by immunoblot to extracts from root tissue (Fig. 4). These data are most consistent with the identification of the 33 kDa, 50 kDa, and 65 kDa immunoreactive proteins as MtPRP1, MtPRP2 and MtPRP3, respectively. MtPRP4 also migrates more slowly than expected for its predicted amino acid sequence (88 kDa observed vs. 62 kDa predicted), and the aberrant migration was confirmed by transgenic expression in hairy root tumors (Fig. 4).

Some contribution to the anomalously slow migration of the PRP proteins might be made by heavy glycosylation of the MtPRPs, as was the case for a PRP extracted from cultured bean cells (Millar et al. 1992). The 42 kDa bean PRP was ~ 32% carbohydrate, glycosylated by extensin-type side chains containing primarily arabinosyl and galactosyl sugars. To detect extensin-like glycosylation in the medic root PRPs, protein gel blots containing immunopurified PRP1 and PRP2 were probed with the JIM11 monoclonal antibody shown to recognize extensin-type glycosyl side chains (Casero et al. 1998). No immunoreactivity with MtPRP1 or MtPRP2 was observed, though JIM11 does recognize other medic root molecules (data not shown).

Solubility of PRPs in root cell walls

The cellular localization of these PRPs was examined using traditional cell fractionation experiments. A crude "cell wall" fraction was isolated from root tissue homogenates by differential centrifugation following extensive washing. As shown in Fig. 5a, high salt extracts of the detergent-washed cell walls (lane 3) contained the same 33 kDa, 50 kDa, and 65 kDa PRP bands that were extracted from whole roots using boiling SDS (lane 5). Insignificant quantities of immunoreactive PRPs were solubilized by subsequent extraction of salt-extracted cell walls with boiling 1% SDS (lane 4), indicating that most of the soluble root PRPs are ionically bound within the cell wall. Significantly greater quantities of MtPRP1 were solubilized when cell walls were extracted with boiling 1% SDS immediately after isolation (lane 5), consistent with a slow oxidative insolubilization of PRP1 in isolated cell walls during the overnight salt extraction. In many experiments, significant amounts of the major PRPs were also found in a soluble crude "cytoplasmic" fraction (1700×*g* supernatant) (lane 1). Since all of these "cytoplasmic" immunoreactive PRPs were found in the 100,000×*g* pellet (Fig. 5b), "cytoplasmic" PRPs probably represent either PRPs bound to small wall fragments that were not

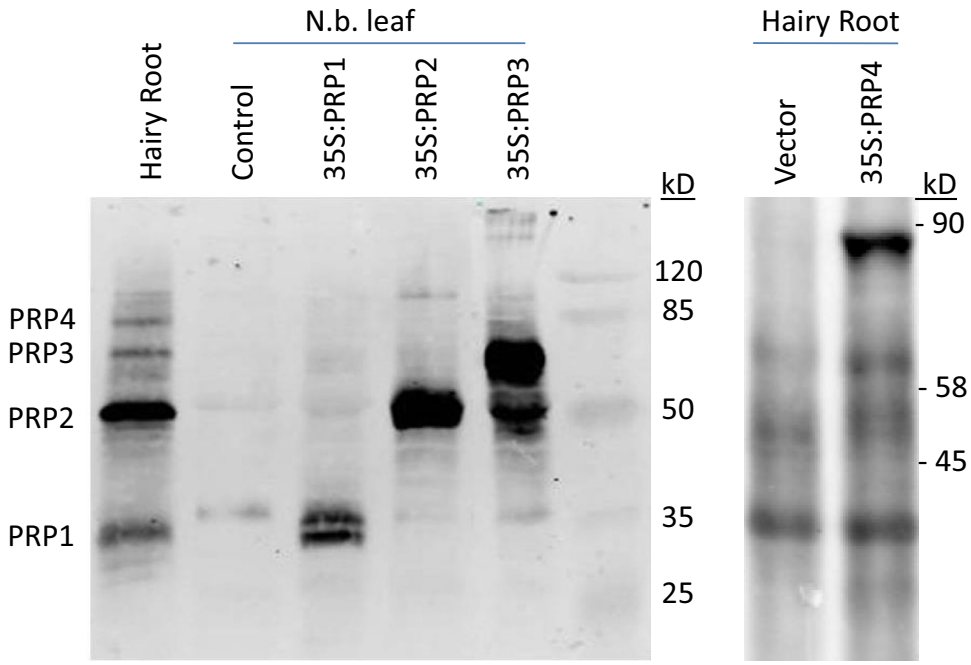

Fig. 4 Immunoblots of transiently expressed PRPs in *N. benthamiana* leaf and *M. truncatula* hairy root tumors, probed with Ab383 (anti-POVH/YK)

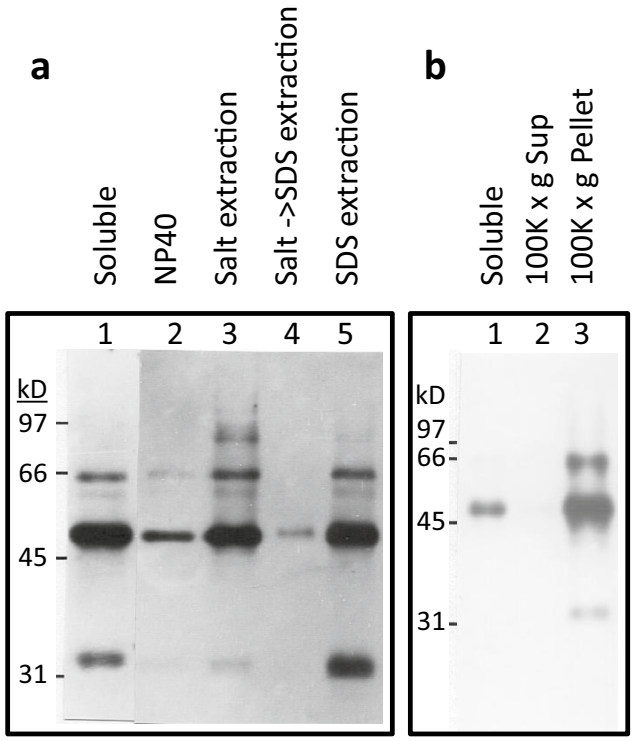

Fig. 5 Fractionation of PRPs detected by anti-SbPRP2. **a** Total soluble fraction (lane 1), 0.1% NP40 wash of cell wall (lane 2), 2 M NH_4Ac, 5 mM ascorbate extraction of cell wall (lane 3), 2% SDS extraction of pellet following salt extraction (lane 4), 2% SDS extraction of cell wall without prior salt extraction (lane 5). **b** Differential centrifugation of soluble cellular proteins. Approximately 1 mg of the soluble fraction was centrifuged for 1 h at 100,000×*g*. All lanes contain 2 µg protein based on BCA assay

efficiently removed by the initial low speed centrifugation, or vesicle-bound PRPs in transit to the extracellular matrix. In some experiments, faint ladders of smaller immunoreactive polypeptides were associated with the two major root PRPs (Fig. 3). However, the relative abundance of this ladder of bands was usually very low, varied between different experiments, and increased with tissue age and long term storage of cell wall extracts at 4 °C. These observations are consistent with these minor PRP-related bands representing discrete degradation products of the major immunoreactive PRPs, as was previously suggested in soybean (Datta and Marcus 1990).

Previous studies with cell cultures showed that the major PRP secreted by legume cells rapidly insolubilized into cell walls, and that the rate-limiting reactant in this oxidative crosslinking was H_2O_2 (Bradley et al. 1992; Otte and Barz 1996). Although treatment of growing medic roots with H_2O_2 also eventually led to a complete loss of all of the major soluble PRPs (data not shown), PRPs could be extracted under alkaline conditions if not subjected to crosslinking treatments (Suppl. Fig. 3). The predicted pIs of the PRPs range from 9.52 to 9.87. When the pH is higher than the pI of the proteins, the net charge of the PRPs becomes negative and at highly basic pH the unesterified carboxyl groups of pectins are also negatively charged, disrupting potential electrostatic interactions between the PRPs and pectins. Enhanced extractability of PRPs under alkaline conditions provides evidence that PRPs are ionically bound to cell wall pectins.

PRP deposition is tissue-specific and restricted to specific wall subdomains

Affinity purified antibodies recognizing both major root PRPs were used to localize PRP deposition in Medicago root tissues by immunohistochemistry. In all cases, we also used cell wall autofluorescence to visualize general root anatomy. As shown in Fig. 6a, immunoreactive PRPs were localized in cells walls of root cortical cells, a ring of pericycle cells surrounding the vascular stele, differentiating protoxylem vessels, and outermost regions of the phloem. No antibody labeling was observed in root epidermal cell walls or in other regions of the phloem, and only weak staining was observed in metaxylem vessels. Within the root cortex, the highest levels of wall PRPs were found in the intercellular junctions formed between neighboring cortical cells forming a triangular pattern between every three neighboring cortical cells (Fig. 6b). In longitudinal sections PRPs were seen localized to xylem pit regions, in paired xylem bordered-pits, and excluded from lignified regions (Fig. 6c, d). Background labeling of root tissues using a non-specific rabbit IgG was minimal (Fig. 6e; Suppl. Fig. 4).

Localization of specific PRPs

Although the high homology within this family aided identification of the additional family members, it impaired attempts to analyze localization and function of discrete family members. Furthermore, the highly repetitive nature of these genes has resulted in their absence from, or incorrect annotation in, *M. truncatula* genome builds. Consequently, we screened a BAC library to obtain genomic fragments that could be used to make promoter fusions to beta-glucuronidase (GUS). We found that all four previously identified *PRP* genes are closely linked within a 70 Mb region of chromosome 4 (Fig. 7), such that individual BAC clones encompassed multiple *PRP* genes (Fig. 7a), including three additional *PRP4*-like genes (*PRP4B-D*) and a *PRP4*-like pseudogene lacking a start codon and signal peptide (Suppl. Fig. 5, GenBank accession numbers MN396798, MN396799, MN3967800, and MN396802). The current build of the *M. truncatula* genome (v. 4.0) includes four "extensin-like repeat protein" genes in this region, but none directly match the sequences of the PRP subclones,

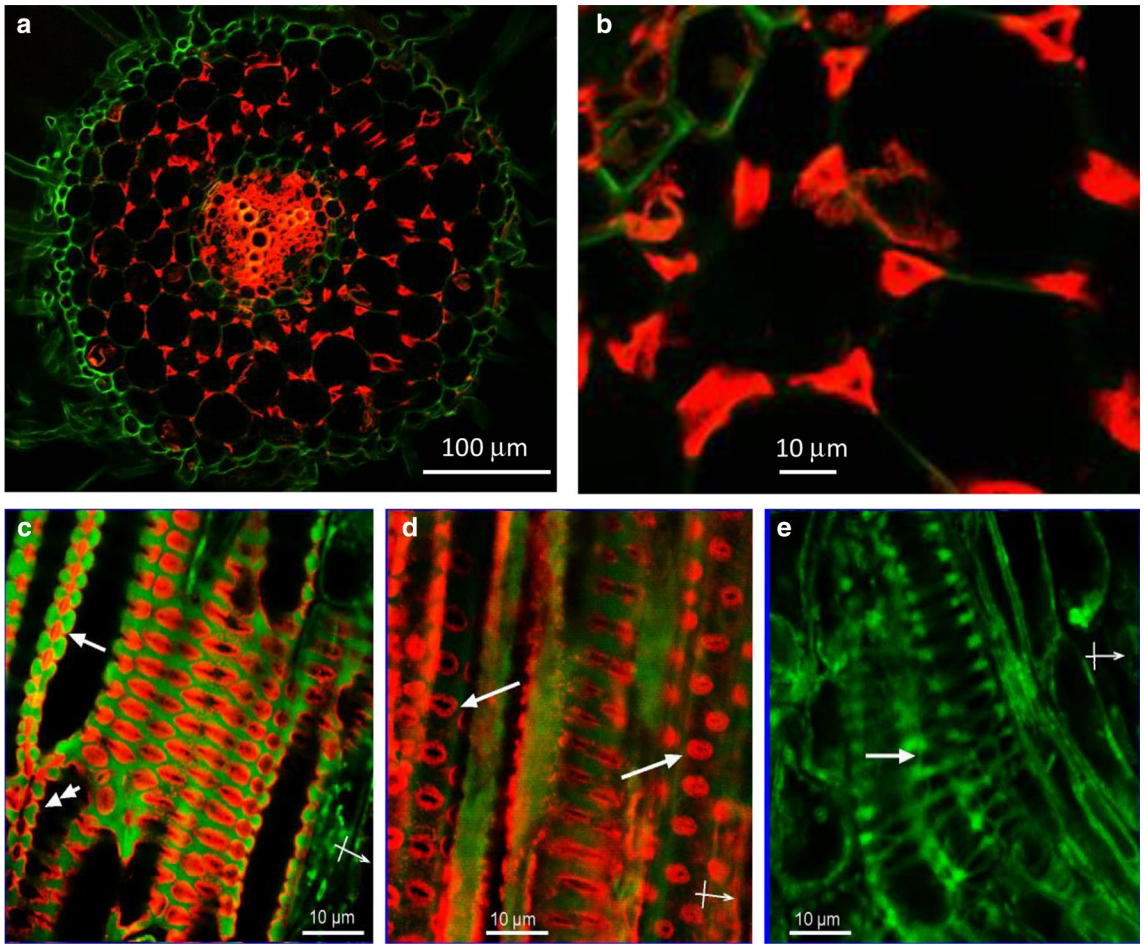

Fig. 6 Confocal microscopy of immunolocalization of PRPs in roots. PRPs are visualized by Ab383 (anti-POVHK/POVYK) and Texas Red-conjugated secondary antibody, phenolic autofluorescence is green. **a** Cross-section showing localization in cell junctions of cortex and stele, **b** high magnification view of cortical cell junctions, **c**, **d** longitudinal sections showing PRP localization in pits and bordered pit-pairs, single arrows indicate pits, double arrow indicates cell wall thickening enveloped by PRPs, **e** differentiating xylem stained with nonimmune rabbit IgG and Texas Red-conjugated secondary antibody

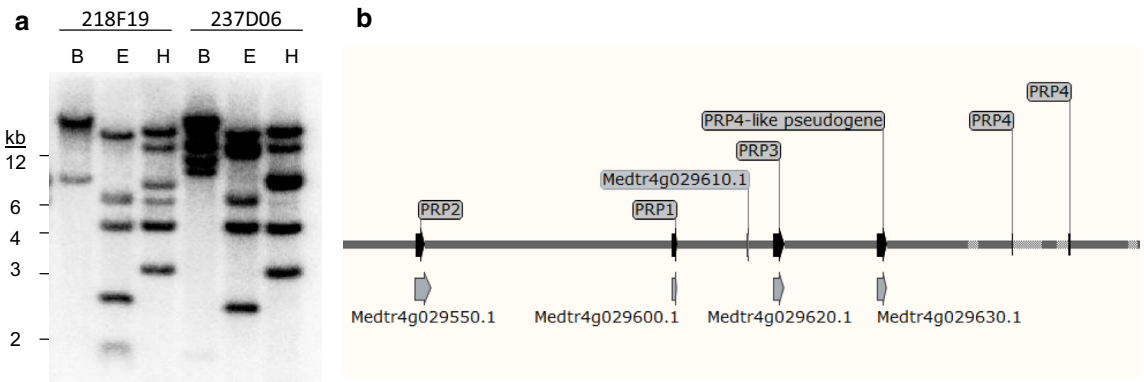

Fig. 7 Genomic organization of PRPs. **a** Bacterial artificial chromosome Southern probed with PRP clone that hybridizes to all PRP family members. BAC clones digested with BamHI (B), EcoRI (E) and HindIII (H). **b** Schematic of chromosome 4 region containing PRP genes based on the *M. truncatula* genome build (v. 4.0) from https://www.medicagogenome.org. None of the "extensin-like" genes in this build show the same number of repeats as in the PRP genomic subclones. Assignments in labels are the closest match. Light grey areas of chromosome are areas of mostly Ns

presumably due to alignment problems in these highly repetitive sequences (Table 1; Suppl. Fig. 6). Medtr4g029550.1 encodes a 311 amino acid protein that resembles PRP2, but lacks 60 codons corresponding to 12 pentapeptide repeats. Medtr4g029600.1 encodes a 221 amino acid protein that is most similar to PRP1, but includes 15 extra codons (3 extra pentapeptide repeats). Medtr4g029620.1 encodes a 379 amino acid protein that resembles PRP3 but lacks 55 codons corresponding to 11 pentapeptide repeats. Medtr4g029630.1 is predicted to encode a 218 amino acid protein that resembles PRP4, but includes only 30 PP-containing pentapeptide repeats and a much shorter leader sequence. None of the full-length PRP4 genes appear in this build, so no corresponding gene names are shown in Fig. 7b, but flanking sequences place them near extended regions of Ns in this genome build.

Analysis of the putative promoter regions for the PRP genes identified potential regulatory motifs including cis-acting elements for response to auxin, cytokinin, light, Myb and HD-Zip transcription factors, and various organ specific response elements (Table 3). The only elements found in all 4 PRP gene family members were those for cytokinin response, Myb and three nodule specific elements. *Agrobacteria* carrying promoter-GUS fusions including between 0.86 and 4.7 kb of upstream sequence were transformed into *M. truncatula* to make hairy root tumors displaying localization of promoter activity for each family member.

PRP1pro:GUS and *PRP2pro:GUS* show nearly identical expression patterns, with GUS activity in the cortex, vascular tissue, and emerging and established root meristems (Fig. 8a–f). *PRP3pro:GUS* is expressed primarily in the endodermis and/or pericycle, vascular tissue and emerging lateral root meristems. Compared to the other family members, *PRP3* expression in established meristems is significantly reduced (Fig. 8g–i). Although *PRP4* was previously shown to be highly expressed in nodules but only weakly expressed in roots (Wilson et al. 1994), the *PRP4* promoter is active in the cortex and xylem as well as established and emerging lateral roots of hairy root tumors. However, *PRP4* expression is weaker at the tip of the meristem (Fig. 8j–l).

Table 3 Conserved *cis* elements found in putative cloned PRP promoter sequences identified by PLACE

PLACE#	PLACE Name	Motif	Category	PRP1	PRP2	PRP3	PRP4
S000370	CATATGGMSAUR	CATATG	Auxin		✓	✓	✓
S000270	ARFAT	TGTCTC	Auxin		✓	✓	✓
S000024	ASF1MOTIFCAMV	TGACG	Auxin / Light				✓
S000454	ARR1AT	NGATT	Cytokinin	✓	✓	✓	✓
S000226	BOXCPSAS1	CTCCCAC	Light (-)		✓		
S000482	SORLIP1AT	GCCAC	Light /Root		✓		✓
S000486	SORLIP5AT	GAGTGAG	Light / Root				✓
S000483	SORLIP2AT	GGGCC	Light +	✓			✓
S000422	TGTCACACMCUCUMISIN	TGTCACA	Fruit				✓
S000314	RAV1AAT	CAACA	Root	✓	✓	✓	✓
S000315	RAV1BAT	CACCTG	Root				✓
S000461	NODCON1GM	AAAGAT	Nodule	✓	✓	✓	✓
S000467	OSE1ROOTNODULE	AAAGAT	Nodule	✓	✓	✓	✓
S000462	NODCON2GM	CTCTT	Nodule	✓	✓	✓	✓
S000468	OSE2ROOTNODULE	CTCTT	Nodule	✓	✓	✓	✓
S000318	ATHB2ATCONSENSUS	CAATSATTG	Generic				✓
S000371	ATHB5ATCORE	CAATNATTG	Generic				✓
S000180	MYBST1	GGATA	Generic	✓	✓	✓	✓
S000474	SITEIIATCYTC	TGGGCY	Meristem				✓
S000352	BS1EGCCR	AGCGGG	Vascular				✓
S000510	XYLAT	ACAAAGAA	Vascular	✓			✓
N/A	N/A	AATTT	Nodule	✓	✓	✓	✓

Color coded by broad category: red = hormone regulated, yellow = light regulated, green = organ-specific, purple = generic transcription factor, blue = tissue-specific

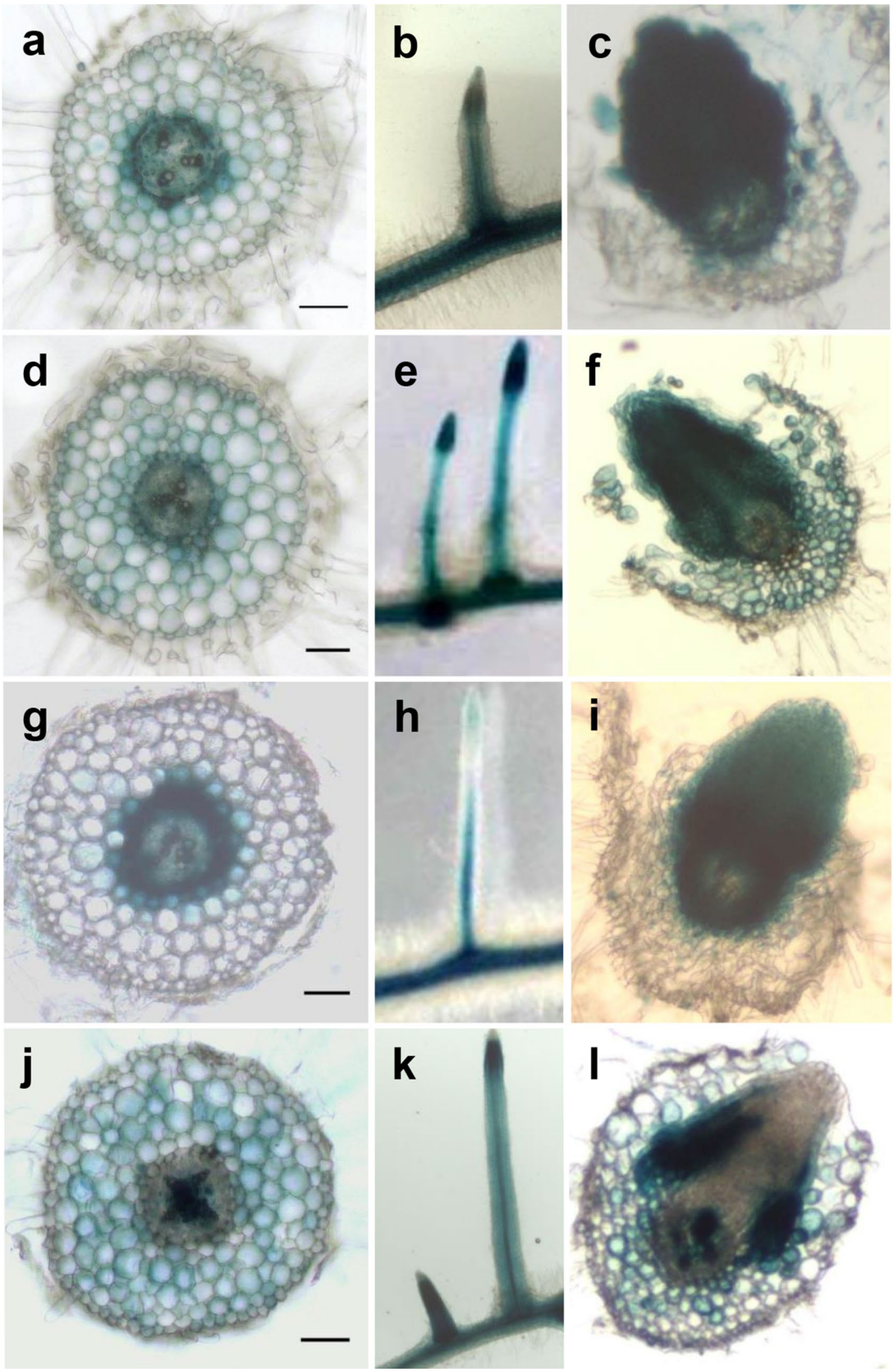

Fig. 8 PRPpro:GUS expression in *Medicago truncatula* hairy roots. Scale bar is 50 µm. **a**–**c** PRP1, **d**–**f** PRP2, **g**–**i**: PRP3, **j**–**l**: PRP4. **a**, **d**, **g**, **j** Cross sections through mature roots; **b**, **e**, **h**, **k** lateral roots; **c**, **f**, **i**, **l** emerging lateral roots

Because it is not possible to test expression in other organs using hairy root tumors, we also constructed transgenic *Arabidopsis* plants to determine whether the promoter specificity was conserved. As in the hairy root tumors, expression of *PRP3pro:GUS* was limited to roots, but reduced in the meristem (Suppl. Fig. 7a–e). As expected based on the EST data, *PRP4pro:GUS* is expressed in siliques (seed pod walls), but not the seeds of *Arabidopsis* (Suppl. Fig. 7j). *PRP4pro:GUS* is also not expressed in the roots of *Arabidopsis* seedlings (Suppl. Fig. 7f–g), possibly reflecting a difference between true roots and hairy root tumors.

PRP knockdown effects on root development

Having determined that hairy root tumors express the three major root-expressed PRPs in specific locations, we sought to test their functions by using RNAi constructs to knock down expression of individual family members. A hairpin RNA construct with 146 bp of the 3′ UTR of MtPRP1 was cloned into pHellsgate and used to create *M. truncatula* hairy roots via *Agrobacterium rhizogenes*-mediated transformation. Although the 3′ UTR is non-repetitive, there was still 76% homology between the 3′ UTRs of MtPRP1 and MtPRP2 in the region cloned in the hairpin construct. Consequently, the MtPRP1 RNAi construct resulted in knockdown of both PRP1 and PRP2 (Suppl. Fig. 8a). Consistent with the observed activity of PRP1 and PRP2 promoters in the cortex and vascular tissue, knockdown of these genes greatly reduced cortical staining with the anti-PRP antibody, but left robust staining within the stele (Fig. 9a, b). Concomitant with the reduced PRP accumulation in the cortex, the cells of the outer cortex varied widely in size and were no longer tightly appressed, suggesting that the PRPs in the cell junctions are important for maintaining cortical structure.

A similar approach, using a 168 bp fragment specific to the 3′ UTR of MtPRP3, was used for additional knockdown experiments. In this case, the knockdown construct had a relatively specific effect on PRP3 accumulation (Suppl. Fig. 8b). As in the PRP1/2 knockdowns, immunostaining of PRP3 was lost in the cortex and enhanced in the stele. However, in addition to distorting cortical cell structure, knockdown of PRP3 drastically reduced growth and viability of the hairy root tumors (Fig. 9c, d). Although transformation with the PRP3 RNAi construct produced tumors at a similar frequency to those produced by the empty vector, the survival rate under selection for maintenance of the transgene was only 7% for the PRP3 knockdown vs. 90% for the empty vector.

Discussion

Genomic organization and expansion of the PRP family

Repetitive PRPs have been described in several legume species and the expression of PRP genes has been well studied in legume stems, cell cultures, and seed coats (Creelman et al. 1992; Datta et al. 1989; Hong et al. 1989; Suzuki et al. 1993a, b; Wyatt et al. 1992; Ye et al. 1991). Fully or partially annotated genome data is available for eleven members of the legume family: *M. truncatula,* chickpea (*Cicer arietinum*), *Lotus japonicus*, soybean (*Glycine max*), Pigeon pea (*Cajanus cajan*), pea (*Pisum sativum*), common bean (*Phaseolus vulgaris*), Mung bean (*Vigna radiata*), Lupin (*Lupinus angustifolius* L.), and two species congeneric with peanut, *Arachis duranensis* and *A.ipaensis* (Bertioli et al. 2016; Dash et al. 2016; Kang et al. 2015; Kreplak et al. 2019; Li et al. 2012) and transcript data (ESTs) is available for several others. Although the closest homologs of the *M. truncatula* PRPs are present in *Trifolium* and *Lotus* species, additional related PRP genes are found in other legumes, ranging from one to six genes in a given species (Supp Fig. 9). In contrast to the distribution of the soybean PRP genes across the genome (two are linked while the other two are on two distinct chromosomes), five of the six *PRP* genes in *P. vulgaris* are linked, and all of the *M. truncatula PRP* genes are linked.

The similarities among the *M. truncatula* PRPs, as well as their close proximity, orientation and almost complete lack of intervening ORFs in the genome, suggest that they arose due to relatively recent tandem duplication events. Despite their similarities, analysis of the pentapeptide repeat content of these seven PRPs suggests they differ in their propensity to form covalent crosslinks via tyrosine residues within the cell wall. The shorter PRPs have higher proportions of tyrosine-containing repeats, and therefore "crosslinking ability" (Table 2), which could suggest that the expansion of the PRP family in *M. truncatula* has allowed for the fine tuning of protein cross-linking in the cell wall.

PRP localization

We used cDNA clones encoding three repetitive *M. truncatula* PRPs and antisera raised against a synthetic PRP domain to investigate cell wall PRPs in seedling roots of a model legume species used for studies of host-microbe symbiosis. *MtPRP1, MtPRP2* and *MtPRP3* represent three of eight closely related members of a gene family in medic that also includes the early nodulin genes *MtENOD12* and

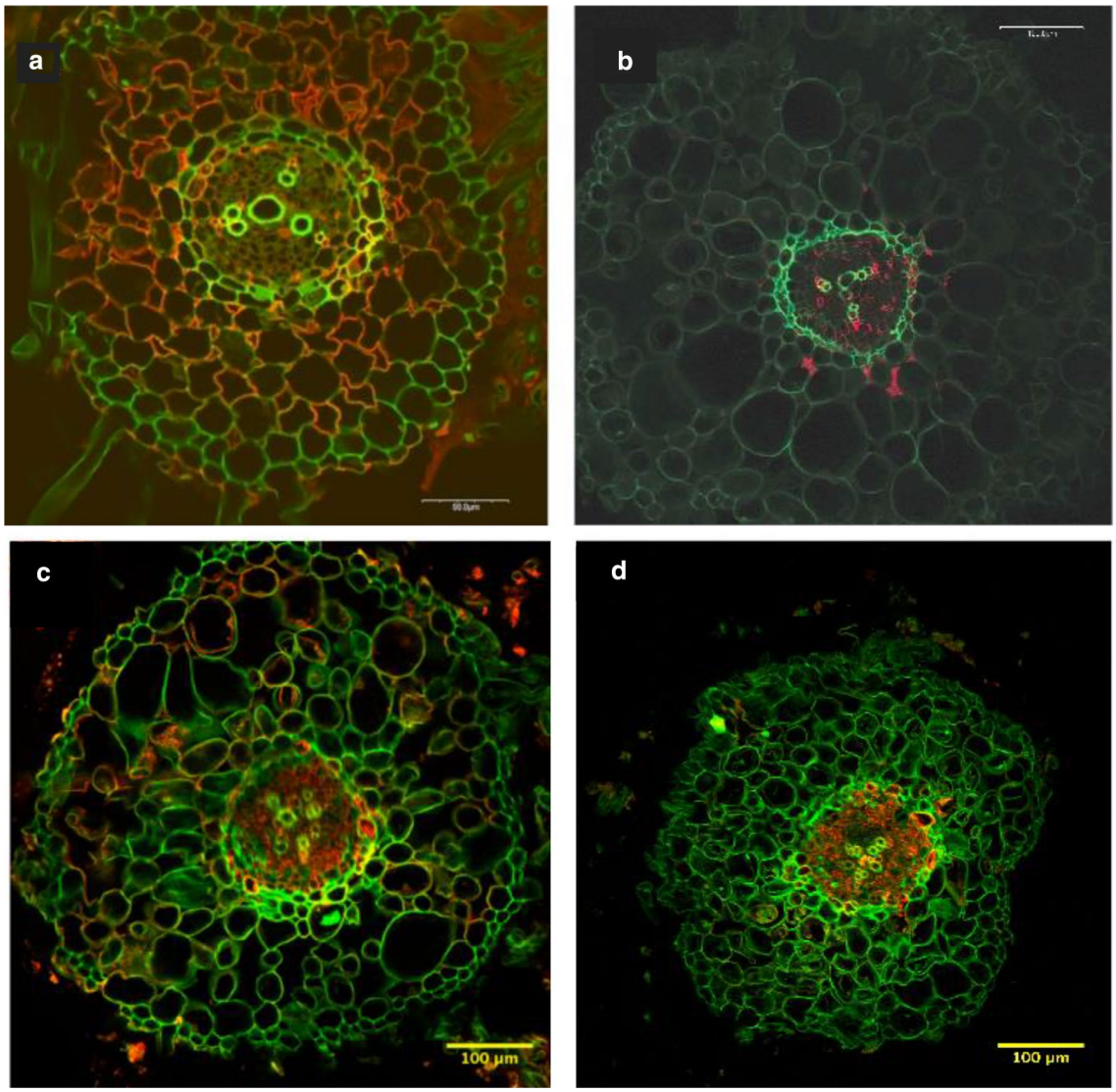

Fig. 9 Confocal microscopy of hairy root tumor cross-sections stained with anti-PRP antibody, Ab383 (red) and showing autofluorescence of the phenolic compounds in the cell wall (green). **a** Empty vector control, **b** MtPRP1 KD, **c**, **d** MtPRP3KD roots

the *MtPRP4* subfamily. Hybridization, RT-PCR and EST analyses identified the major PRP transcripts expressed in medic roots as *MtPRP1, MtPRP2,* and *MtPRP3*, and all three of these PRP transcripts accumulated to the highest levels in roots compared to aerial organs of medic seedlings (hypocotyl, leaf, and cotyledon) (Wilson et al. 1994).

Three major root PRPs, with apparent molecular masses of 33 kDa, 50 kDa, and 65 kDa were recognized by affinity-purified antibodies raised against a synthetic repetitive PRP motif. The levels of these polypeptides generally paralleled the previously reported levels of the major PRP transcripts in different seedling organs (Wilson et al. 1994) in that PRP1 and PRP2 were more abundant than PRP3. Transient expression of all four PRPs in either *N. benthamiana* leaves or *M. truncatula* hairy root tumors showed that these wall proteins migrate at significantly higher apparent molecular weights in SDS-PAGE experiments compared to the sizes predicted from the cDNA sequences (Wilson and Cooper 1994), but consistent with the sizes observed in root tissue.

In general, proline-rich polypeptides have been found to migrate with exaggerated size on SDS-PAGE (Datta et al. 1989; Proft et al. 1995). This discrepancy between predicted and apparent sizes of the major medic PRPs is most likely due to an unusual conformation adopted by the repetitive PRPs that lowers the amount of dodecyl sulfate binding compared to globular proteins. Molecular modeling studies and preliminary physical experiments using synthetic PRP domains are consistent with an unusual polypeptide conformation for legume cell wall PRPs that is distinct from the polyproline II helix (J.B. Cooper and J.T. Gerig, unpublished

results). This conformation may resemble contiguous tandem repeats of the polyproline, beta-turn helix proposed for other proline-rich polypeptides (Matsushima et al. 1990).

Affinity purified antibodies recognizing the major medic root PRPs were used to localize PRPs in tissues of the mature regions of medic seedling roots. Results of these experiments demonstrate that PRPs are abundantly deposited in the intercellular junctions between neighboring root cells, particularly in the root cortex, in walls of the root pericycle cells and endodermis, and in the developing xylem and phloem tissues (Fig. 6). Ye et al. (1991) previously reported a similar pattern of PRP deposition in soybean roots. The triangular pattern of immunostaining in the intercellular junction regions suggests that PRPs may be localized to the borders of the expanded middle lamellae formed between any three neighboring cortical cells. This pattern is similar to localization patterns reported for xyloglucan (Moore and Staehelin 1988), a minor HRGP extension (Swords and Staehelin 1993), and an HRGP epitope recognized by the JIM12 monoclonal antibody. In contrast, it differs from the patterns reported for acidic pectins and other HRGP epitopes that were deposited inside the expanded middle lamella region of intercellular junctions (Moore and Staehelin 1988; Swords and Staehelin 1993), an extracellular domain previously shown to contain acidic pectins (Willats et al. 2001) and the putative crosslinking enzyme diamine oxidase (Wisniewski et al. 2000).

Localization and roles of specific PRPs were analyzed by promoter fusions to the GUS reporter and knockdown of individual or closely related family members. Although promoters for all three major root PRPs were active in the stele, promoters of PRP1 and especially PRP2 were also active in the cortex. Consistent with this, RNAi knockdown of PRP1 and PRP2 resulted in loss of cortical PRP accumulation and increased PRP accumulation in the stele except for mature xylem, suggesting that PRP3 expression increased to compensate for loss of PRP1/2. Although PRP3 promoter activity in the cortex is relatively weak, PRP3 knockdown also led to decreased cortical PRPs and increased PRP accumulation in the stele, again consistent with compensatory changes in accumulation of the various PRP family members. In all cases, reduced expression in the cortex was correlated with highly variable cell size and more gaps between cells. However, unlike PRP1 and PRP2, PRP3 appeared to be essential for continued root growth because knockdown lines had greatly reduced viability. Recently, a poplar PRP was also found to be preferentially expressed in developing vascular tissue, and to regulate secondary wall formation in *P. deltoides* (Li et al. 2019).

The absence of PRP deposition in root epidermal tissue contrasts with conclusions based on gene fusion data in other species. Suzuki et al. (1993a, b) demonstrated that *SbPRP*1 promoter sequences are sufficient to express a GUS reporter gene in epidermal cells of tobacco and cowpea roots. This difference may indicate either that PRP expression pattern in medic roots differs from the pattern in soybean and cowpea roots, and/or that expression of promoter-GUS gene fusions in heterologous plant systems are not sufficient to reach conclusions regarding tissue-specific gene expression (Taylor 1997).

Potential roles of PRPs in root development

Taken together, these data demonstrate that the junctions occurring between conjoining root cortical cells have a discontinuous molecular composition consisting of a triangular "core" (composed primarily of pectic gel polymers) sheathed by distinct cell wall containing PRPs and HRGPs. From supercellular tissue perspective, the system of connected intercellular junction regions throughout the root cortex should function to integrate the mechanical properties of the entire root cortex. Such a wall architecture, based on strong triangular girders, might provide the strength needed to resist the crushing external physical pressures exerted on the cortex as roots expand in diameter and push down through the soil matrix. Loss of these structures in the cortex tissue of the knockdown lines is accompanied by increased expression in the stele. Although increased PRP3 in the stele is enough to maintain growth of hairy root tumors in liquid culture, the remaining PRP1 and PRP2 in the PRP3 knockdown lines is not sufficient for viability, indicating that these highly similar proteins are functionally distinct.

Extractability under alkaline conditions demonstrated that at least a portion of the PRPs deposited in cortical cell junctions exist in a soluble form, possibly ionically bound to pectins. Since early responses to pathogen attack include rapid oxidative crosslinking of pre-existing wall PRPs (Bradley et al. 1992; Otte and Barz 1996), the PRPs located in the intercellular junction regions may represent an important site of early defense against pathogens. In this context, studies on the resistance response of lettuce with an incompatible bacterial pathogen demonstrated that H_2O_2 was generated in the intercellular junction regions, and that infection by the incompatible pathogen was restricted to these sites (Hammond-Kosack and Jones 1996).

The expanded middle lamellar regions in the junctions between root cortical cells can also become filled with air during root development (Esau 1977). While the molecular details of the development of these intercellular spaces is poorly defined, the resulting air channels are thought to provide oxygen to subterranean root tissues. In symbiotic nodules formed on pea roots, PRP deposition was observed in the intercellular junctions between nodule parenchyma cells (Sherrier and VandenBosch 1994); this tissue expresses ENOD2, encoding a proline-rich protein only distantly related to the PRPs, that has been proposed

to play a role in regulating oxygen diffusion into root nodules (Franssen et al. 1992). By analogy, since PRPs are present in the molecular "linings" of the cortical air channels, they might play a role in controlling the movement of gases out of these intercellular air channels and into root cortical cells.

In the root vasculature, immunostaining of PRPs was heaviest in the walls of differentiating xylem located in the protoxylem region and in the phloem region known to develop into phloem fiber cells at the outermost regions of root phloem (Esau 1965). The deposition of PRPs in walls of lignifying vascular tissues was previously reported in soybean seedlings (Ye et al. 1991) and in pea roots subtending symbiotic root nodules (Sherrier and VandenBosch 1994), and a potential involvement of PRPs in lignification has been discussed (Sherrier and VandenBosch 1994; Showalter 1993; Ye et al. 1991).

In summary, our data begins to characterize a gene family encoding repetitive cell wall PRPs in the important model legume *M. truncatula*. Three of the seven PRP genes are strongly expressed in seedling roots. All of these major wall PRPs are secreted as soluble molecules that can be oxidatively insolubilized by H_2O_2. Expression of all three root PRP genes was shown to be tissue-specific, and deposition of wall-bound PRPs was localized to the intercellular junctions between neighboring cells in root cortical and pericycle tissue, and to the lignifying cell types of the root vascular system. Studies on other wall structural gene products (HRGPs and GRPs) have also implicated a role for extracellular matrix proteins and glycoproteins in vascular development (reviewed by Showalter 1993) and in root development generally. Although reaching a complete understanding of the interactions of PRPs with themselves and with other wall structural elements will likely prove a difficult task, it is clear that much more information will be necessary to understand how these structural molecules function in plant cell walls, and how their role in wall architecture is involved in the development of roots and the differentiation of specific tissues.

Acknowledgements Portions of this work were supported by the Department of Energy Biosciences program (DE-FG03-95ER20192) to JBC, and by a UC Biotechnology Training Grant. We gratefully thank Dr. Mary Tierney (University of Vermont) for a gift of anti-soybean PRP2 antibodies, Dr. Monte Radeke for help with peptide synthesis and advice on producing anti-peptide antibodies, Dr. Brian Matsumoto and Dr. Mary Raven for advice and training on the confocal microscope and for use of a vibratome, and Laura Polacco, Lucas Hanscom, Scott Spivack, Kim O'Keefe, Julia Dubiel, Mario Guzman, and Emily Garcia for general laboratory assistance.

Author contributions JBC conceived and obtained funding for the project. JBC and RRF conceived and supervised experiments. BJE, NCS, NH, CW and MAS conceived and performed experiments. All authors contributed to writing or providing feedback on the manuscript.

References

Albenne C, Canut H, Jamet E (2013) Plant cell wall proteomics: the leadership of *Arabidopsis thaliana*. Front Plant Sci. https://doi.org/10.3389/fpls.2013.00111

Allison LA, Kiss GB, Bauer P, Poiret M, Pierre M, Savouré A, Kondorosi E, Kondorosi A (1993) Identification of two alfalfa early nodulin genes with homology to members of the pea Enod12 gene family. Plant Mol Biol 21:375–380

Averyhart-Fullard V, Datta K, Marcus A (1988) A hydroxyproline-rich protein in the soybean cell wall. Proc Natl Acad Sci USA 85:1082–1085

Barker D, Pfaff T, Moreau D, Groves E, Ruffel S, Lepetit M, Whitehand S, Maillet F, Nair R, Journet E-P (2006) Growing *M. truncatula*: choice of substrates and growth conditions. In: Mathesius U, Journet E, Sumner L (eds) The *Medicago truncatula* handbook, Noble Research Institute, Ardmore

Bertioli DJ, Cannon SB, Froenicke L, Huang G, Farmer AD, Cannon EK, Liu X, Gao D, Clevenger J, Dash S, Ren L, Moretzsohn MC, Shirasawa K, Huang W, Vidigal B, Abernathy B, Chu Y, Niederhuth CE, Umale P, Araújo AC, Kozik A, Do Kim K, Burow MD, Varshney RK, Wang X, Zhang X, Barkley N, Guimarães PM, Isobe S, Guo B, Liao B, Stalker HT, Schmitz RJ, Scheffler BE, Leal-Bertioli SC, Xun X, Jackson SA, Michelmore R, Ozias-Akins P (2016) The genome sequences of *Arachis duranensis* and *Arachis ipaensis*, the diploid ancestors of cultivated peanut. Nat Genet 48:438–446

Boisson-Dernier A, Chabaud M, Garcia F, Bécard G, Rosenberg C, Barker D (2001) *Agrobacterium rhizogenes*-transformed roots of *Medicago truncatula* for the study of nitrogen-fixing and endomycorrhizal symbiotic associations. Mol Plant–Microbe Interact 14:695–700

Bradley DJ, Kjellbom P, Lamb CJ (1992) Elicitor- and wound-induced oxidative cross-linking of a proline-rich plant cell wall protein: a novel, rapid defense response. Cell 70:21–30

Casero PJ, Casimiro I, Knox JP (1998) Occurrence of cell surface arabinogalactan-protein and extension epitopes in relation to pericycle and vascular tissue development in the root apex of four species. Planta 204:252–259

Cassab GI (1998) Plant cell wall proteins. Ann Rev Plant Physiol Plant Mol Biol 49:281–309

Church GM, Gilbert W (1984) Genomic sequencing. Proc Natl Acad Sci USA 81:1991

Creelman RA, Tierney ML, Mullet JE (1992) Jasmonic acid/methyl jasmonate accumulate in wounded soybean hypocotyls and modulate wound gene expression. Proc Natl Acad Sci USA 89:4938

Dash S, Campbell J, Cannon E, Cleary A, Huang W, Kalberer S, Karingula V, Rice A, Singh J, Umale P, Weeks N, Wilkey A, Farmer A, Cannon S (2016) Legume information system (LegumeInfo.org): a key component of a set of federated data resources for the legume family. Nucl Acids Res 44:D1181–D1188

Datta K, Marcus A (1990) Nucleotide sequence of a gene encoding soybean repetitive proline-rich protein 3. Plant Mol Biol 14:285–286

Datta K, Schmidt A, Marcus A (1989) Characterization of two soybean repetitive proline-rich proteins and a cognate cDNA from germinated axes. Plant Cell 1:945–952

Duruflé H, Hervé V, Balliau T, Zivy M, Dunand C, Jamet E (2017) Proline hydroxylation in cell wall proteins: Is it yet possible to define rules? Front Plant Sci 8:1802

Esau K (1965) Plant anatomy. Wiley, New York

Esau K (1977) Anatomy of the seed plants. Wiley, New York

Feinberg AP, Vogelstein B (1983) A technique for radiolabeling DNA restriction endonuclease fragments to high specific activity. Anal Biochem 132:6–13

Fowler TJ, Bernhardt C, Tierney ML (1999) Characterization and expression of four proline-rich cell wall protein genes in Arabidopsis encoding two distinct subsets of multiple domain proteins. Plant Physiol 121:1081–1091

Franssen HJ, Nap J-P, Gloudemans T, Stiekema W, Van Dam H, Govers F, Louwerse J, Van Kammen A, Bisseling T (1987) Characterization of cDNA for nodulin-75 of soybean: a gene product involved in early stages of root nodule development. Proc Natl Acad Sci USA 84:4495–4499

Franssen HJ, Vijn I, Yang WC, Bisseling T (1992) Developmental aspects of the rhizobium-legume symbiosis. Plant Mol Biol 19:89–107

Fry SC (1982) Isodityrosine, a new cross-linking amino acid from plant cell-wall glycoprotein. Biochem J 204:449–455

Gamas P, Debellé F, Berges H, Godiard L, Niebel A, Journet E, Gouzy J (2006) *Medicago truncatula* cDNA and genomic libraries. In: Mathesius U, Journet E, Sumner L (eds) The *Medicago truncatula* handbook, Noble Research Institute, Ardmore

Garcia J, Barker D, Journet E-P (2006) Seed storage and germination. In: Mathesius U, Journet E, Sumner L (eds) The *Medicago truncatula* handbook, Noble Research Institute, Ardmore

Hale I, Matsumoto B (1993) Resolution of subcellular detail in thick tissue sections: immunohistochemical preparation and fluorescence confocal microscopy. Methods Cell Biol 38:289–324

Hammond-Kosack KE, Jones JD (1996) Resistance gene-dependent plant defense responses. Plant Cell 8:1773–1791

Hong JC, Nagao RT, Key JL (1989) Developmentally regulated expression of soybean proline-rich cell wall protein genes. Plant Cell 1:937–943

Hong JC, Nagao RT, Key JL (1990) Characterization of a proline-rich cell wall protein gene family of soybean. J Biol Chem 265:2470–2475

Jefferson RA, Kavanagh TA, Bevan MW (1987) GUS fusions: beta-glucuronidase as a sensitive and versatile gene fusion marker in higher plants. EMBO J 6:3901–3907

Journet E-P, El-Gachtouli N, Vernoud V, de Billy F, Pichon M, Dedieu A, Arnould C, Morandi D, Barker DG, Gianinazzi-Pearson V (2001) *Medicago truncatula* ENOD11: A Novel RPRP-encoding early nodulin gene expressed during mycorrhization in arbuscule-containing cells. Mol Plant–Microbe Interact 14:737–748

Kang YJ, Satyawan D, Shim S, Lee T, Lee J, Hwang WJ, Kim SK, Lestari P, Laosatit K, Kim KH, Ha TJ, Chitikineni A, Kim MY, Ko JM, Gwag JG, Moon JK, Lee YH, Park BS, Varshney RK, Lee SH (2015) Draft genome sequence of adzuki bean *Vigna angularis*. Sci Rep 5:8069

Keller B (1993) Structural cell wall proteins. Plant Physiol 101:1127–1130

Kieliszewski MJ, Lamport DTA (1994) Extensin: Repetitive motifs, functional sites, post-translational codes, and phylogeny. Plant J 5:157–172

Kleis-San Francisco SM, Tierney ML (1990) Isolation and characterization of a proline-rich cell wall protein from soybean seedlings. Plant Physiol 94:1897–1902

Kreplak J, Madoui M-A, Cápal P, Novák P, Labadie K, Aubert G, Bayer PE, Gali KK, Syme RA, Main D, Klein A, Bérard A, Vrbová I, Fournier C, d'Agata L, Belser C, Berrabah W, Toegelová H, Milec Z, Vrána J, Lee H, Kougbeadjo A, Térézol M, Huneau C, Turo CJ, Mohellibi N, Neumann P, Falque M, Gallardo K, McGee R, Taran B, Bendahmane A, Aury J-M, Batley J, Le Paslier M-C, Ellis N, Warkentin TD, Coyne CJ, Salse J, Edwards D, Lichtenzveig J, Macas J, Doležel J, Wincker P, Burstin J (2019) A reference genome for pea provides insight into legume genome evolution. Nat Genet 51:1411–1422

Li J, Dai X, Liu T, Zhao PX (2012) LegumeIP: an integrative database for comparative genomics and transcriptomics of model legumes. Nucl Acids Res 40:D1221–D1229

Li S, Zhang Y, Ding C, Gao X, Wang R, Mo W, Lv F, Wang S, Liu L, Tang Z, Tian H, Zhang J, Zhang B, Huang Q, Lu M, Wuyun T-n, Hu Z, Xia Y, Su X (2019) Proline-rich protein gene PdPRP regulates secondary wall formation in poplar. J Plant Physiol 233:58–72

Lindstrom JT, Vodkin LO (1991) A soybean cell wall protein is affected by seed color genotype. Plant Cell 3:561–571

Löbler M, Hirsch AM (1993) A gene that encodes a proline-rich nodulin with limited homology to PsENOD12 is expressed in the invasion zone of *Rhizobium meliloti*-induced alfalfa root nodules. Plant Physiol 103:21–30

Marcus A, Greenberg J, Averyhart-Fullard V (1991) Repetitive proline-rich proteins in the extracellular matrix of the plant cell. Physiol Plant 81:273–279

Matsushima N, Creutz CE, Kretsinger RH (1990) Polyproline, β-turn helices. Novel secondary structures proposed for the tandem repeats within rhodopsin, synaptophysin, synexin, gliadin, RNA polymerase II, hordein, and gluten. Proteins Struct Funct Bioinform 7:125–155

Millar DJ, Slabas AR, Sidebottom C, Smith CG, Allen AK, Bolwell GP (1992) A major stress-inducible Mr-42000 wall glycoprotein of French bean (*Phaseolus vulgaris* L.). Planta 187:176–184

Moore PJ, Staehelin LA (1988) Immunogold localization of the cell-wall-matrix polysaccharides rhamnogalacturonan I and xyloglucan during cell expansion and cytokinesis in *Trifolium pratense* L.; implication for secretory pathways. Planta 174:433–445

Murashige T, Skoog F (1962) A revised medium for rapid growth and bio assays with tobacco tissue cultures. Physiol Plant 15:473–497

Nakagawa T, Suzuki T, Murata S, Nakamura S, Hino T, Maeo K, Tabata R, Kawai T, Tanaka K, Niwa Y, Watanabe Y, Nakamura K, Kimura T, Ishiguro S (2007) Improved gateway binary vectors: high-performance vectors for creation of fusion constructs in transgenic analysis of plants. Biosci Biotechnol Biochem 71:2095–2100

Nam Y-W, Penmetsa RV, Endre G, Uribe P, Kim D, Cook DR (1999) Construction of a bacterial artificial chromosome library of *Medicago truncatula* and identification of clones containing ethylene-response genes. Theor Appl Genet 98:638–646

Newman AM, Cooper JB (2007) XSTREAM: a practical algorithm for identification and architecture modeling of tandem repeats in protein sequences. BMC Bioinform 8:382

Newman AM, Cooper JB (2011) Global analysis of proline-rich tandem repeat proteins reveals broad phylogenetic diversity in plant secretomes. PLoS ONE 6:e23167

Otte O, Barz W (1996) The elicitor-induced oxidative burst in cultured chickpea cells drives the rapid insolubilization of two cell wall structural proteins. Planta 200:238–246

Otte O, Barz W (2000) Characterization and oxidative in vitro cross-linking of an extensin-like protein and a proline-rich protein purified from chickpea cell walls. Phytochem 53:1–5

Perlick AM, Pühler A (1993) A survey of transcripts expressed specifically in root nodules of broadbean (*Vicia faba* L.). Plant Mol Biol 22:957–970

Pichon M, Journet EP, Dedieu A, de Billy F, Truchet G, Barker DG (1992) *Rhizobium meliloti* elicits transient expression of the early nodulin gene ENOD12 in the differentiating root epidermis of transgenic alfalfa. Plant Cell 4:1199–1211

Proft T, Hilbert H, Layh-Schmitt G, Herrmann R (1995) The proline-rich P65 protein of *Mycoplasma pneumoniae* is a component of the Triton X-100-insoluble fraction and exhibits size polymorphism in the strains M129 and FH. J Bacteriol 177:3370–3378

Sainsbury F, Lomonossoff GP (2014) Transient expressions of synthetic biology in plants. Curr Opin Plant Biol 19:1–7

Scheres B, Van De Wiel C, Zalensky A, Horvath B, Spaink H, Van Eck H, Zwartkruis F, Wolters A-M, Gloudemans T, Van Kammen A, Bisseling T (1990) The ENOD12 gene product is involved in

the infection process during the pea-Rhizobium interaction. Cell 60:281–294
Schultz C, Harrison M (2008) Novel plant and fungal AGP-like proteins in the *Medicago truncatula–Glomus intraradices* arbuscular mycorrhizal symbiosis. Mycorrhiza 18:403–412
Sherrier DJ, VandenBosch KA (1994) Localization of repetitive proline-rich proteins in the extracellular matrix of pea root nodules. Protoplasma 183:148–161
Showalter AM (1993) Structure and function of plant cell wall proteins. Plant Cell 5:9–23
Suzuki H, Fowler T, Tierney M (1993a) Deletion analysis and localization of SbPRP1, a soybean cell wall protein gene, in roots of transgenic tobacco and cowpea. Plant Mol Biol 21:109–119
Suzuki H, Wagner T, Tierney ML (1993b) Differential expression of two soybean (*Glycine max* L.) proline-rich protein genes after wounding. Plant Physiol 101:1283–1287
Swords K, Staehelin LA (1993) Complementary immunolocalization patterns of cell wall hydroxyproline-rich glycoproteins studied with the use of antibodies directed against different carbohydrate epitopes. Plant Physiol 102:891–901
Taylor CB (1997) Promoter fusion analysis: an insufficient measure of gene expression. Plant Cell 9:273–275
Verdonk JC, Hatfield RD, Sullivan ML (2012) Proteomic analysis of cell walls of two developmental stages of alfalfa stems. Front Plant Sci. https://doi.org/10.3389/fpls.2012.00279
Wang T, Zabotina O, Hong M (2012) Pectin-cellulose interactions in the Arabidopsis primary cell wall from two-dimensional magic-angle-spinning solid-state nuclear magnetic resonance. Biochemistry 51:9846–9856
Watson BS, Lei Z, Dixon RA, Sumner LW (2004) Proteomics of *Medicago sativa* cell walls. Phytochemistry 65:1709–1720
Wesley SV, Helliwell CA, Smith NA, Wang M, Rouse DT, Liu Q, Gooding PS, Singh SP, Abbott D, Stoutjesdijk PA, Robinson SP, Gleave AP, Green AG, Waterhouse PM (2001) Construct design for efficient, effective and high-throughput gene silencing in plants. Plant J 27:581–590
White PB, Wang T, Park YB, Cosgrove DJ, Hong M (2014) Water-polysaccharide interactions in the primary cell wall of *Arabidopsis thaliana* from polarization transfer solid-state NMR. J Am Chem Soc 136:10399–10409
Willats WGT, McCartney L, Mackie W, Knox JP (2001) Pectin: cell biology and prospects for functional analysis. Plant Mol Biol 47:9–27
Wilson RC, Cooper JB (1994) Characterization of PRP1 and PRP2 from *Medicago truncatula*. Plant Physiol 105:445–446
Wilson RC, Long F, Maruoka EM, Cooper JB (1994) A new proline-rich early nodulin from *Medicago truncatula* is highly expressed in nodule meristematic cells. Plant Cell 6:1265–1275
Wise AA, Liu Z, Binns AN (2006) Three methods for the introduction of foreign DNA into Agrobacterium. In: Wang K (ed) Agrobacterium protocols. Humana Press, Totowa, pp 43–54
Wisniewski J-P, Rathbun EA, Knox JP, Brewin NJ (2000) Involvement of diamine oxidase and peroxidase in insolubilization of the extracellular matrix: implications for pea nodule initiation by *Rhizobium leguminosarum*. Mol Plant–Microbe Interact 13:413–420
Wyatt RE, Nagao RT, Key JL (1992) Patterns of soybean proline-rich protein gene expression. Plant Cell 4:99–110
Ye Z-H, Song Y-R, Marcus A, Varner JE (1991) Comparative localization of three classes of cell wall proteins. Plant J 1:175–183
Ziemer MA, Mason A, Carlson DM (1982) Cell-free translations of proline-rich protein mRNAs. J Biol Chem 257:11176–11180